

Mott Scattering of Polarized Muons*

MARCEL BARDON, PAOLO FRANZINI,[†] AND JULIET LEE
Columbia University, New York, New York

(Received January 31, 1962)

An experimental determination has been made of the helicity of muons from π^- decays and the cross sections for scattering from lead by Mott scattering. With $(2.0 \pm 0.3) \times 10^8$ muons incident on the scatterers, a left-right asymmetry of -0.090 ± 0.031 was measured for a total of 1163 ± 60 scattering events. Extensive checks indicated negligible systematic asymmetries. The sign of the asymmetry shows a positive helicity for the negative muon in pion decay in agreement with $V-A$ theory. Agreement of the magnitude of the asymmetry and of the number of events with the ones predicted for the experimental arrangement (0.081 ± 0.001 and 1210 ± 220 , respectively) confirms the results of other experiments which have indicated a purely electromagnetic behavior for muon scattering. This experiment, at an average momentum transfer of 110 Mev/c, has the added interest of being the only measurement of the Mott scattering of transversely polarized fermions in this momentum transfer region.

I. INTRODUCTION

PREVAILING considerations in the theory of weak interactions¹ have led to renewed interest in the helicity of the muon in pion decay, i.e., in the helicity of the associated neutrino. Although in $V-A$ theory² the negative muon emitted in the decay $\pi^- \rightarrow \mu^- + \bar{\nu}$ is predicted to have a helicity $+1$ (fully right-handed) in the rest system of the pion, recent postulations of the existence of two neutrinos—one associated with the muon and the other with the electron—might lead to the possibility of opposite helicity. The experiment³ was designed to measure this quantity by Mott scattering of transversely polarized muons. In addition, it yields information bearing on the validity of considering the muon as a “heavy electron” in its behavior in nuclear scattering.

The method used was to measure the left-right asymmetry in backward scattering of transversely polarized muons from lead. The expected distribution is of the form $a(\theta)[1+b(\theta)P \cos \varphi]$, where P is the polarization of the muon along the y axis (in the usual right-handed coordinate system with the z axis along the direction of the initial muon momentum), and θ and φ are the polar and azimuthal angles for the final momentum direction. The evaluation of the energy dependent terms a and b for the experimental arrangement is described in Sec. IV. It was necessary that the experimental setup be fully optimized for maximum yield and effect (Secs. II and III) because of the low intensity of transversely polarized muons and the very small scattering probability.

The result of this measurement of -0.090 ± 0.031 for the left-right asymmetry (Sec. V) leads to the conclusion

* Research supported in part by the Office of Naval Research and the United States Atomic Energy Commission.

[†] Fulbright Fellow. Present address: University of Pisa, Pisa, Italy.

¹ See, for example, B. Pontecorvo, J. Exptl. Theoret. Phys. (U.S.S.R.) **37**, 1751 (1959); [translation: Soviet Phys.—JETP **37**(10), 1236 (1960)]; and also T. D. Lee and C. N. Yang, Phys. Rev. Letters **4**, 307 (1960).

² R. P. Feynman and M. Gell-Mann, Phys. Rev. **109**, 139 (1958).

³ A preliminary description of the helicity measurement has been given in Phys. Rev. Letters **7**, 23 (1961).

of positive helicity for the μ^- in $\pi-\mu$ decay (Appendix II). This same conclusion is reached in experiments involving the Møller scattering of high-energy longitudinally polarized muons by aligned electrons in magnetized iron with cosmic rays⁴ and recently with laboratory produced muons at the CERN proton synchrotron.⁵

The measured number of scattering events agrees well with those calculated (Sec. IV) by assuming the muon to be a Dirac particle scattering in the static Coulomb field of an extended nuclear charge distribution of the “Fermi” shape,⁶ with parameters determined from electron scattering data.⁷ (Magnetic scattering corrections and nuclear model dependence of the scattering are negligible, Sec. IV.)

A question had arisen about such a treatment because some cosmic ray experiments⁸ indicated an anomalous behavior in muon-nuclear scattering. This, however, has in fact been cleared up by two subsequent experiments with laboratory produced muons.^{9,10} But of these, one involved small-angle scatterings of 2-Bev muons where the inclusion of inelastic scattering made comparison with theory complicated, and the other was hampered by the lack of events in a high momentum transfer region. This experiment, where the average momentum transfer was 110 Mev/c and which had a negligible amount of inelastic scattering, makes the additional contribution of measuring the magnitude of the asymmetry. The agreement with the calculated value provides further support for the pure electromagnetic behavior of the muon in scattering.

⁴ A. E. Alikhanov *et al.*, J. Exptl. Theoret. Phys. (U.S.S.R.) **38**, 1918 (1960); [translation: Soviet Phys.—JETP **11**, 1380 (1960)].

⁵ G. Backenstoss, B. D. Hyams, G. Knop, P. C. Maria, and U. Stierlin, Phys. Rev. Letters **6**, 415 (1961).

⁶ G. H. Rawitscher, Phys. Rev. **112**, 1278 (1958).

⁷ R. Hofstadter, Ann. Rev. Nuclear Sci. **7**, 231 (1957).

⁸ For a summary of experiments up to 1958, see G. N. Fowler and A. W. Wolfendale, *Progress in Elementary Particle and Cosmic-Ray Physics* (North-Holland Publishing Company, Amsterdam, 1958), Vol. 4, p. 123.

⁹ G. E. Masek, L. D. Heggie, Y. B. Kim, and R. W. Williams, Phys. Rev. **112**, 937 (1961).

¹⁰ P. L. Connolly, J. G. McEwen, and J. Orear, Phys. Rev. Letters **6**, 554 (1961).

II. EXPERIMENTAL ARRANGEMENT

A. Beam

The muons used originated from decays in flight of pions produced in the Nevis synchrocyclotron. Their energy and transverse polarization were chosen by appropriate selection of pion beam energy and muon emission angles.

1. Pion Beam

A study had been made to ascertain the energy range and maximum angular divergence acceptable for this experiment on consideration of the asymmetries and cross sections expected. It was found that moderating the lowest energy pion beam obtainable (≈ 65 Mev) with absorbers to the required 28 Mev, and subsequently collimating and momentum-analyzing, would result in too low an intensity.

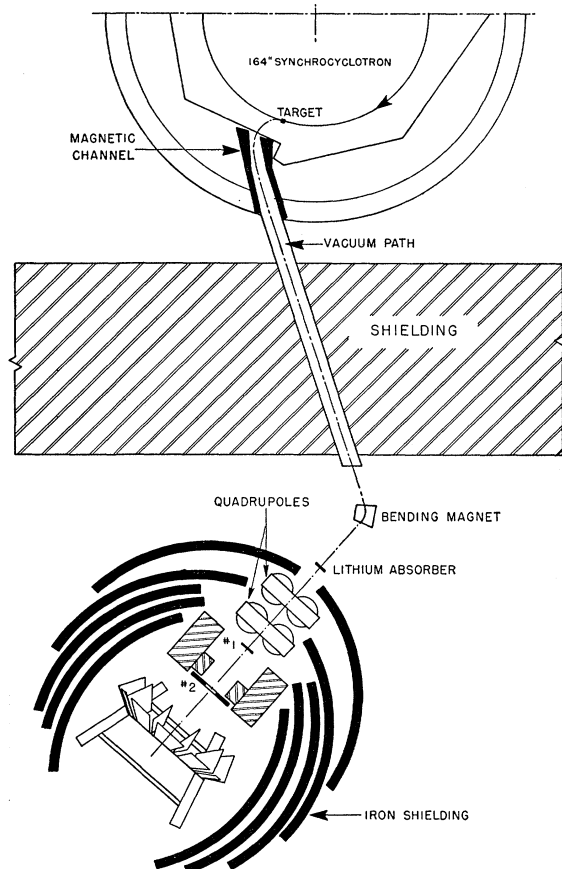


FIG. 1. Plan view of the cyclotron, shielding wall, and experimental area. The beryllium target in the cyclotron vacuum chamber is the source of pions for which is shown a trajectory through the vacuum path in the magnetic channel and shielding wall, the bending magnet, the lithium moderator which slows down the pions from 43 to 28 Mev, the quadrupole focusing magnets, and the well shielded experimental area. The 9-in. diameter No. 1 counter with the No. 2 collimating counter (6-in. by 8-in. elliptical hole) in anticoincidence define the pion beam.

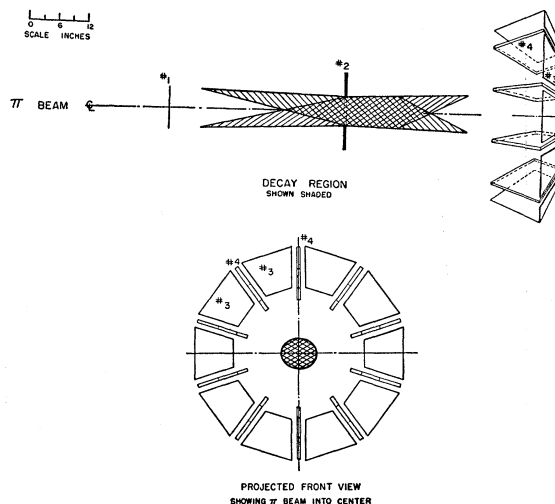


FIG. 2. Experimental setup showing the annular arrangement of the 10 sets of counters and lead scatterers. The pion beam is defined by the No. 1 counter (9 in. diameter, $\frac{1}{8}$ in. thick) with the No. 2 counter (6-in. by 8-in. elliptical hole) in anticoincidence. The shaded part indicates the region of the pion beam from which decays in flight give muons which reach the scatterers. In this schematic diagram only the plastic scintillators are indicated. The lead scatterers (2 g/cm^2 thick) were directly behind, and of the same shape as, each No. 3 scintillator (trapezoids 9-in. high, with 6-in. and 11-in. bases, $\frac{1}{8}$ -in. thick). The No. 4 counters (same dimensions but $\frac{3}{4}$ -in. thick) detected muons scattering backwards through 100° to 155° on the average. On the bottom, is shown a projected front view of the wheel arrangement, looking along the direction of the incoming pion beam.

The arrangement chosen involved installing a magnetic channel to shield lower energy pions from the fringing field of the cyclotron, and a recessed window to permit installation of the channel close enough to the target in the circulating proton beam. The layout is shown in Fig. 1. Iron shims were placed near the proton beam to cancel out perturbations produced by the channel. The resulting (5- \times -5-in.) pion beam at the exit of the bending magnet was 25 000 pions/sec at 43 ± 1.5 Mev. This beam was moderated to the required 28 ± 2.5 Mev by 3 in. of lithium placed at the common focus of the bending magnet and a pair of quadrupoles. The pion beam was defined by this system and two counters: a circular 9-in. diameter counter (No. 1) placed at the exit of the quadrupole system, and 3 ft further, in anticoincidence, a large counter (No. 2) with a 6- by 8-in. elliptical hole. The pions emerged with an angular divergence of $\pm 2^\circ$ and an intensity of 11 000/sec. The electron contamination was measured to be $\approx 20\%$ of the total beam.

2. Muon Beam

Muons which result from decay in flight of pions have their energy and polarization determined by the laboratory angle of emission and the pion energy, as discussed in Appendix I. The target positions, orientation, and distance from the pion beam were chosen taking into account the extent of the beam, its angular di-

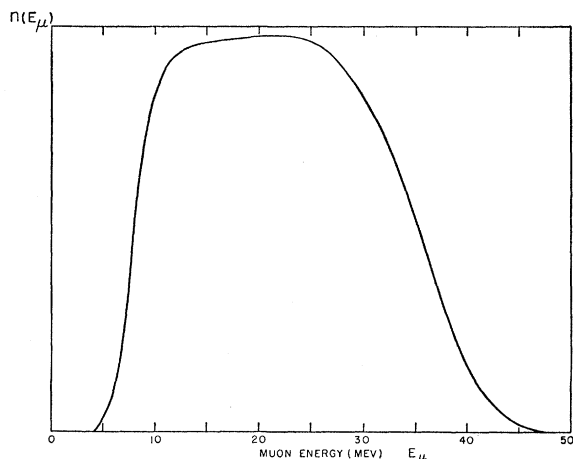


FIG. 3. Energy spectrum of the muons incident on the lead scatterers, calculated (Appendix I) for the 28-Mev pion beam (with a ± 2.5 Mev spread) and the geometry of the experimental arrangement.

vergence, and energy spread, and the extent of the target. The relevant parameters are shown in Fig. 2. In this way, a decay region about 5 ft long was defined; with a minimum angle of emission set by the geometry, and a maximum corresponding to the largest decay angle kinematically allowable.

Azimuthal symmetry in the emission of muons about the pion beam direction made it possible to increase the intensity and minimize systematic asymmetries by surrounding the pion beam with ten identical sets of targets and detectors (described in Sec. II B). This arrangement is shown in Fig. 2. These sets were mounted on a wheel which was rotated at frequent intervals to cancel out effects which might result from small deviations from axial symmetry of the pion beam intensity.

The muon energy spectrum for this arrangement and the dependence of polarization on muon energy were calculated as discussed in Appendix I and are shown in Figs. 3 and 4, respectively. The muons resulted from the decay of 7% of the pions, and they had a transverse polarization, averaged over muon energies, of 90%.

3. Evacuated Beam Path and Shielding

The entire path from the cyclotron window to the bending magnet (≈ 25 ft) was evacuated to reduce multiple scattering of the pions. The rest of the path was lined with helium filled polyethylene bags with walls 0.003 in. thick, so that multiple scattering did not contribute any correction to the angular distribution of the muons.

Precautions were taken to shield the equipment from stray radiations as the real counting rate was expected to be low. Thick iron shielding was placed on all sides and on the top, the back being left free for the passage of the pion beam. Blocks of borax-paraffin were used in the front wall to reduce the low-energy neutron background.

B. Target and Detector Assembly

A schematic diagram of the equipment is shown in Fig. 2.

1. Targets and Target Thickness

The ten lead targets used for scattering the muons were arranged symmetrically in an annular ring about the pion beam as axis. These are 2-g/cm² thick isosceles trapezoids whose sides were radial from the center of the pion beam. They were 9 in. high, with bases 6 and 11 in., and were tilted toward the pion beam axis at 25° to a plane perpendicular to the pion beam. They were thus perpendicular to the mean direction of the muons emitted from the pion beam. The thicknesses were uniform to 1%.

The thickness of the lead scatterers was chosen to be 2 g/cm² after careful consideration of the many factors involved. A very thin target would result in too low a rate of scattering while a thick one would give a large contribution of multiple Coulomb scattering of the muons. This would result in a loss of detectable polarization. The usable target thickness is also limited by the residual range of the backward scattered muon. A most important consideration is plural scattering. Historically, the observation of the predicted asymmetry in Mott scattering of transversely polarized electrons was delayed nearly ten years because the effect was obliterated by the contamination of plural scattering from too thick targets. The problem is even greater in this experiment because the low rate necessitates the use of large targets and detectors. This difficulty arises mainly because of the steep dependence of the asymmetry (Fig. 7) and the cross section (Fig. 6) on angle and energy; e.g., it follows that a double scattering of two medium angles at low energy could be as frequent (while showing little asymmetry) as a single scattering at higher energy. This could affect the measurement of

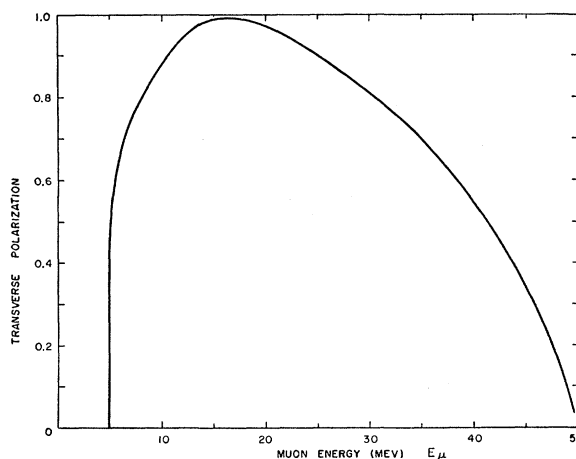


FIG. 4. Dependence of the transverse polarization on the energy of the muons incident on the lead scatterers, as calculated (Appendix I) for the experimental arrangement used.

both cross section and asymmetry considerably. Analysis shows that for the chosen thickness of 2 g/cm^2 of lead scatterer, double scattering contributed $\approx 30\%$ of the events, but that of these, 80% were due to scattering by a large angle followed by a small-angle scattering, and thus hardly diluted the asymmetry.

2. Detectors

All the detectors were plastic scintillators viewed through lucite light pipes by 6655A ten-stage photomultipliers. In front of each lead scattering target there was a $\frac{1}{16}$ -in. thick plastic scintillator of the same shape as the target (the No. 3 counters of Fig. 2). At each side of the targets were the No. 4 counters, $\frac{3}{4}$ -in. thick scintillators, trapezoidal in shape, 9 in. high with 6- and 11-in. bases. Of those muons which scattered back from the lead through angles ranging on the average from 100° to 155° , and which would reach the No. 4 counters, about 80% would stop in these thick counters. This arrangement had the particular virtue that a No. 4 counter, which detected scatterings to the right for one set, was also the one to detect those to the left for the adjacent set. The counters were all aligned with respect to the targets and to each other to $1/64$ in., which resulted in a negligible contribution to the uncertainties in cross section and asymmetry.

3. Muon Shields

In order to prevent muons from entering the No. 4 counters directly rather than after scattering from the lead, $\frac{3}{4}$ -in. thick copper strips were placed along the beam edge of these counters. The scattering from these copper shields was calculated to give a negligible contribution to the counting rate. These shields intercepted 27% of the muon beam.

C. Electronic Logic

A scattered muon event was defined by the following sequence of signals and electronic coincidences:

- (1) A pion passing through No. 1 and through the hole in No. 2 was counted as a $(1)\bar{2}$ anticoincidence.
- (2) A $1\bar{2}$ in coincidence with a signal in one of the No. 3 counters gave an incident muon signal: $(1\bar{2})(3)$.
- (3) A muon scattered backwards into one of the No. 4 counters was detected as a $(1\bar{2}3)(4)$ coincidence.
- (4) The $1\bar{2}34$ signal does not, however, uniquely define a scattering event. With this requirement alone, a major part of the counting rate would be due to mesonic x rays from muons which stop in the lead (Sec. V B), the x ray being converted there or in the No. 4 counter. For this reason, it was required that the muons stop in the No. 4 counters ($\approx 80\%$ of them do) and give a delayed count from the $\mu \rightarrow e$ decay. Thus the $1\bar{2}34$ signal was used to open a delayed gate during which single counts in No. 4 were put in coincidence with the $1\bar{2}34$ signals. These, then were counted as events.

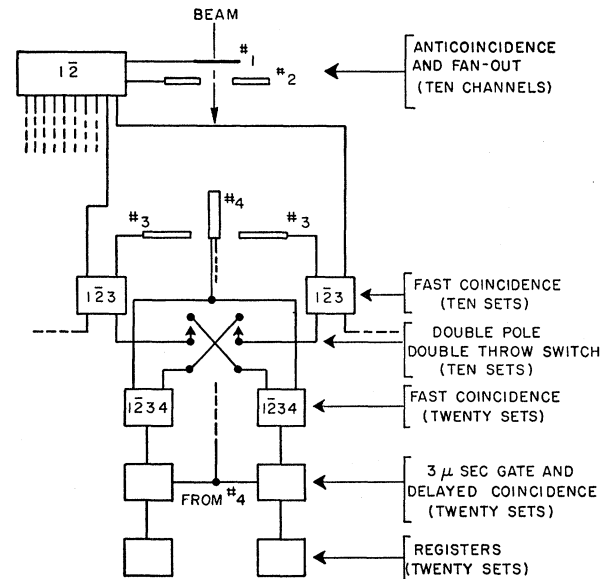


Fig. 5. Simplified schematic diagram of the electronics. The $1\bar{2}$ signal corresponding to a pion in the beam is distributed by a pulse shaping fan-out system to ten sets of fast coincidence circuits, together with a signal from one of the No. 3 counters in each. The $1\bar{2}3$ outputs define a muon incident on a particular one of the ten scatterers. The backward scattering is observed as a fast coincidence with a No. 4 counter. The two outputs from each $1\bar{2}3$ are distributed through double-pole, double-throw relays allowing the interchange of the circuits which give the $1\bar{2}34$ coincidences for "right" and "left" scattering events. An identifying muon signature is obtained by counting the electron from $\mu \rightarrow e$ decay (from a second output of each No. 4 counter) in delayed coincidence with a $4\text{-}\mu\text{sec}$ gate opened by the appropriate $1\bar{2}34$ prompt coincidence. Fast amplifiers on the No. 3 and $1\bar{2}3$ outputs as well as discriminators and pulse shapers on the No. 4 signal for the delayed counts are not shown on the diagram. All fast coincidences were made with specially designed tunnel diode circuits. (Reference 11.)

A simplified block diagram of the electronics is shown in Fig. 5. The convenient use of the large number of circuits was made possible by having them transistorized. All the fast coincidences were made with a specially designed simple tunnel diode circuit.¹¹

The $1\bar{2}$ signal was distributed to 10 two-fold coincidence circuits with a signal from a No. 3 counter in each. The resolving time was made $\approx 10 \text{ nsec}$ to accept the spread in time of arrival of muons of various energies from decays of pions at various distances past the No. 1 counter. The ten output signals, $1\bar{2}3$, had the timing of the pulses from the No. 3 counters and represented a muon incident on a particular one of the ten sets of scatterers.

Each $1\bar{2}3$ signal was sent to two of 20 other twofold coincidence circuits, with each of two adjacent No. 4 counters. These were set to have $\approx 5 \text{ nsec}$ resolving time to cover the spread in time of muons reaching the No. 4 counters after scattering. The resulting $1\bar{2}34$ signals ("gates") were counted, and were used to open a $3.0\text{-}\mu\text{sec}$ gate delayed by $0.10 \mu\text{sec}$. A second signal from

¹¹ Paolo Franzini, Rev. Sci. Instr. 32, 1222 (1961).

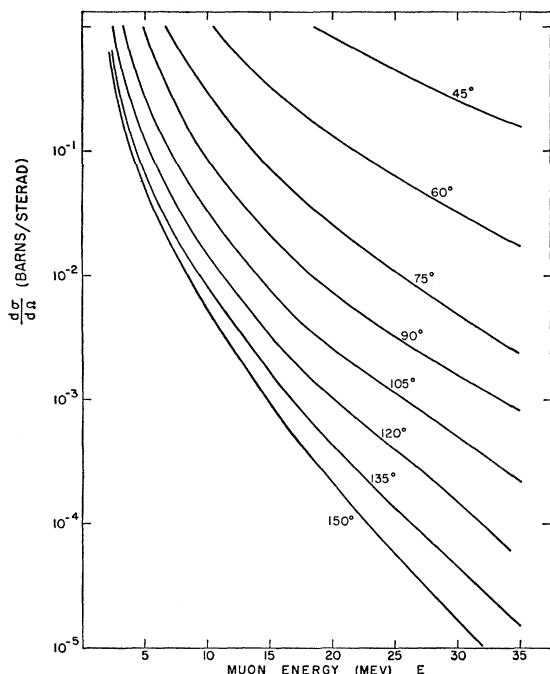


FIG. 6. Scattering cross section for negative muons from lead, as a function of muon energy and for various scattering angles, calculated for Coulomb scattering from an extended nuclear charge distribution of "Fermi shape" with parameters determined from electron scattering data (references 6, 7, 14).

No. 4 was discriminated in amplitude, shaped, and put in coincidence with the gate. These are the "event" signals, corresponding to a backward scattered muon which stopped in either a left or a right No. 4 counter and there identified itself as a muon by decaying into an electron during the gate open time.

In order that the same chain of electronic circuits be used for counting both left and right scattering events, ten sets of double-pole, double-throw relays were used to interchange at regular intervals the sequence of circuits which gave the ($\bar{1}\bar{2}34$) left and right event signals.

III. EXPERIMENTAL PROCEDURE

A. Beam Measurements

The beam parameters size, angular distribution, energy spread, and electron contamination are given in Sec. II A. The resulting flux incident on each of the 10 lead targets was 60 muons/sec, with energy spectrum and polarization as shown in Figs. 3 and 4. From the energy and angular distribution of the π^- beam, we compute that not more than one π^- in four thousand would scatter into the target region.¹² Furthermore, such π^- contamination would only give rise to "gates" and of a negligible amount, hence constitute no contribution to the rate of spurious events.

¹² H. S. Snyder and W. T. Scott, Phys. Rev. **76**, 220 (1949).

B. Equalization of Electronic Channels

A first-order cancellation of systematic asymmetries is achieved by the switching of left and right channels for each set, and from the closed wheel arrangement of the detectors; that is, effects for "left" and "right" channels cancel only when the counting rates are of the same magnitude. For this reason all the sequences of circuits were set so they had similar efficiencies in adjacent channels. This was done by using a pulser consisting of two 6655 A photomultipliers viewing the same small piece of plastic scintillator exposed to a Sr^{90} source. This gave two pulses with spectra similar to the outputs of the No. 3 and No. 4 counters. A third pulse was sent through the $\bar{1}\bar{2}$ circuit and fan-out system to give the same $\bar{1}\bar{2}$ signals as would be obtained with the beam. Thus the $\bar{1}\bar{2}3$ and $\bar{1}\bar{2}34$ coincidences could be simulated and all twenty channels set to count similar rates. The differences were about 1% and contributed negligibly to the uncertainties.

C. Setting No. 3 Counter Voltages

The voltages on the target counters (No. 3) were set as low as possible to cut down the background rate, while retaining full sensitivity to the highest energy muons desired (≈ 28 Mev) crossing twice. This was done by making a study of the pulse height vs voltage properties. Then, from the voltage which gave full sensitivity to minimum ionizing particles, the voltage setting was found. Checks were made with pions of 43 Mev, 20 Mev, and with a continuous spectrum of muons. All ten No. 3 counters were set at full efficiency to better than 5%, for muons of 28 Mev or less crossing the scintillator twice. At this setting, $(17 \pm 2.5)\%$ of the incident muons with single traversals were being counted. At various times, the voltages were raised to count the actual number of incident muons as a $\bar{1}\bar{2}3$ signal fully sensitive to muons crossing only once.

D. Setting No. 4 Counter Voltages

Two outputs were taken from each of the No. 4 counters; one for the fast $\bar{1}\bar{2}34$ coincidence and the other for counting electrons in the delayed gate. Since one output was clipped with a shorted line and the second was sent to a discriminator and pulse former, it was possible to set the sensitivities independently for each output.

For the fast clipped signal, the counters were set to be fully sensitive within 10% at the desired cutoff of 6 Mev minimum energy loss for muons, by calibrating with minimum ionizing particles and correcting for the saturation effects of slow particles.

For the second output, in order to have good sensitivity to decay electrons, the discriminators were set to give full efficiency for pulses corresponding to 2-Mev loss in the scintillator. The efficiency for detecting an electron after a muon stopped in the scintillator was computed to be 55% and measured as $(54 \pm 2)\%$.

IV. EXPECTED YIELD

Calculations for the scattering cross section $d\sigma/d\Omega$ and the polarization asymmetry factor S_0 of the negative muons from heavy nuclei, at several values of muon energies, are available from two papers.^{13,6} Both use the Dirac equation, assuming that the potential acting on the muon is that of a static Coulomb interaction arising from an extended charge distribution. Rawitscher, for example, used the "Fermi" model where the "half density" radius and the skin thickness of the distribution were determined by the electron scattering experiments of Hofstadter.⁷ Additional values of $d\sigma/d\Omega$ and S_0 for the muon energies relevant to the present experiment were computed from the same IBM 650 program¹⁴ which yielded the results in reference 6. They are shown in Figs. 6 and 7 as a function of muon energy E and scattering angle θ . The consequences of neglecting such effects as inelastic scattering, nuclear magnetic scattering, quadrupole scattering, etc., in the evaluation of $d\sigma/d\Omega$ and S_0 will be discussed at the end of the present section.

The expected yield is obtained by the integration of $d\sigma/d\Omega$ and S_0 over the parameters of our experimental arrangement. To indicate the various factors involved, we write out, for single scattering, the contribution from an element l of scattering target, as measured through a particular electronic channel j .

This is written in a form which exhibits the dependence on the experimental parameters:

$$W_{ij} \propto \frac{N_0}{A} \int f(E_\mu) dE_\mu \int \sin\theta d\theta d\varphi \times \int \frac{d\sigma[E(l, E_\mu), \theta]}{d\Omega} [1 + S_0(\theta, E) P(E_\mu) \cos\varphi] dl,$$

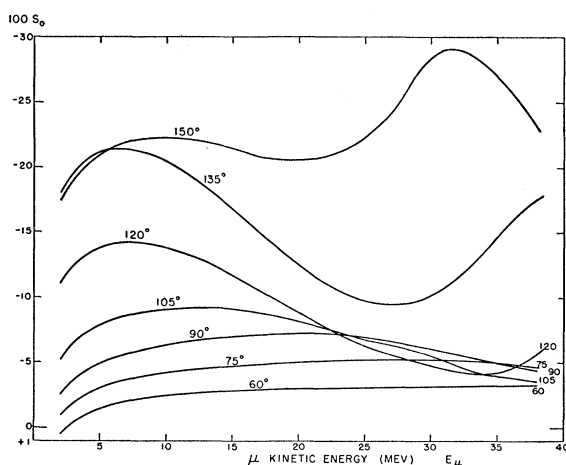


FIG. 7. Polarization asymmetry factor for negative muons scattered from lead, as a function of muon energy and for various scattering angles, calculated as Fig. 6.

¹³ J. Franklin and B. Margolis, Phys. Rev. **109**, 525 (1958).

¹⁴ We are particularly grateful to Dr. G. H. Rawitscher for his kind loan of a computer program which we used in the calculations of scattering probabilities and asymmetries.

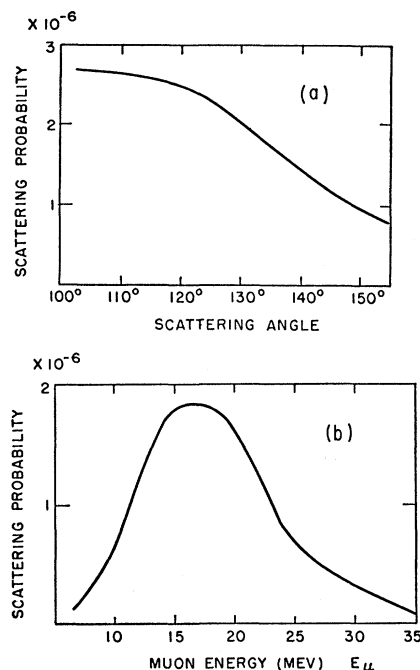


FIG. 8. Probability for single scattering calculated for the experimental arrangement; shown in (a) summed over the muon energies, as a function of scattering angle; and in (b) summed over scattering angles, as a function of muon energy.

where W_{ij} is the probability of scattering, N_0 is Avogadro's number, A is the atomic weight of the scatterer, E_μ is the energy of the incoming muon before penetration of the target, and E is the energy of the muon at scattering. $f(E_\mu)$ is the incoming muon energy distribution as determined by the geometry (Sec. II and Appendix I) and the requirement that the No. 3 counter voltages and the 123 resolving times are such that they do not affect the optimized conditions of the setup, θ and φ are the scattering and azimuthal angles defined in Sec. I. The integration over angles includes the effect of multiple scattering in the lead, which corresponds to an additional angular dependence for the probability of reaching a No. 4 counter. l is the scattering interaction length for which the integration limits are determined both from the target thickness, and from the range requirements for muons to emerge from the lead after scattering at some penetration depth. They must also traverse two scintillators, losing sufficient energy in each to be detected. Hence, l is dependent on the No. 3 and No. 4 counter voltages and on the 1234 coincidence resolving time.

$d\sigma/d\Omega$ is the aforementioned elastic Coulomb differential scattering cross section of a Dirac muon from an extended lead nucleus. It is a function of E and θ , which in turn are functions of the interaction length l and the incoming muon energy E_μ . Its strong dependence on E and θ forecasted a possible great sensitivity of W on E_μ , hence on target thickness; and of W on θ , hence, on geometric alignment. This, however, did not turn out

to be the case as may be seen in Fig. 8 where one or the other parameter has been integrated out.

S_0 is the polarization asymmetry factor defined such that, for a transversely polarized beam, it is the left-right scattering asymmetry; that is, the relative number of scatterings at $\varphi=0$ minus the number at $\varphi=\pi$, divided by the sum of the two scatterings. It is a function of E and θ .

P is the transverse polarization of the muons which, for a given pion energy, is determined by the incoming muon energy E_μ . (See Fig. 4 and Appendix I.)

The main contribution to the expected yield, that due to single scattering, is given by Eq. (2). The analogous expression for double scattering includes products of two $d\sigma/d\Omega$'s and is much more involved, with the complication arising mainly from the fact that the z axis for the second scattering is the final direction of the muon at its first scattering. Contributions from higher-order scattering are negligible. After integrations over the limits corresponding to the experimental arrangement, the total scattering probability is obtained from the W_{ij} for single scattering and the corresponding expression for double scattering by summing over the elements of scattering target and over the electronic channels. The results predicted are:

$$W = (1.1 \pm 0.1) \times 10^{-5}.$$

The asymmetry S is given by the probability of scattering to the right subtracted from the probability of scattering to the left, divided by the sum. The calculation yields for the magnitude of the expected asymmetry:

$$S = 0.081 \pm 0.001.$$

The errors indicated for W and S are due to the uncertainties in the parameters of the experimental setup. A simple argument which relates the sign of S with the polarization (Appendix II) shows that a positive helicity for the muon leads to a negative sign for S .

We also mention here two numbers of some interest: (i) the mean momentum transfer $q = 2p \sin(\theta/2)$, where p is the momentum of the muon at the point of scatter, is 110 Mev/ c ; (ii) the mean scattering cross section is ≈ 2 mb. We note also that it is the very smallness of W , coupled with the relatively low intensity of polarized muons which made this experiment difficult.

For simplicity, the problem of inelastic scattering has so far been treated with the aid of the Born approximation.^{15,16} Favorable arguments had been given¹⁷ for the validity of such a treatment in estimating the contributions. In our experiment, the smallness of the energy transfer (≈ 0.03 Mev to the nucleus as a whole or ≈ 6 Mev, if the energy were to be imparted to a single nucleon) leads to a low inelastic scattering contribution,

and this ultimately justifies the evaluation of an upper limit by the method. Other correction terms also assumed Born approximation type calculations, again acceptable because of the smallness of their effects.

A straightforward application of the formula from the work of Smith¹⁵ (derived with sum rules neglecting nuclear spin effects) predicts an increase of 25% in the number of scatterings from the inclusion of the inelastic scattering. However, it is known from photonuclear effects that the major excitation energies are between 15 and 20 Mev¹⁸ (the "giant resonance"). Therefore, considering that for this experiment the mean muon energy at scattering was ≈ 18 Mev and that a 6-Mev energy loss requirement on the No. 4 counters was imposed, less than one tenth of the inelastically scattered muons would have been detected, reducing the contamination from the inelastic scattering events to $< 2.5\%$.

Nuclear magnetic scattering terms are expected to contribute negligibly because of the low value of the nuclear spin of the lead targets (these were of normal abundance: 56% Pb²⁰⁸, spin 0; 26% Pb²⁰⁶, spin 0; 21% Pb²⁰⁷, spin $\frac{1}{2}$). Adapting the Drell and Schwartz¹⁶ formulation to lead, by using Smith's "two-body correlation" functions, we estimate that the total magnetic scattering corrections do not exceed 2%. Lastly, the quadrupole moment scattering contribution is expected to be nil.¹⁹

V. EXPERIMENTAL RESULTS

The data were taken for 95 hr during which the sequences of circuits for counting left and right scatterings were interchanged every hour, and the wheel arrangement was rotated in a non-coherent manner eleven times. There were 2×10^8 muons incident on the lead scatterers for 4×10^9 pions in the beam. The uncorrected results for the total number of scattering events to the left and to the right are: $N_L = 583$,

TABLE I. Data as obtained for each of the 10 sets, listed under " μ^- scattering." The two other columns show the results of the checks on systematic asymmetries made with scattered π^+ mesons, and with the "gate" counts due to μ -mesonic x rays from muons stopping in the lead scatterers.

Set No.	μ^- Scattering		π^+ Scattering		Gates	
	Left	Right	Left	Right	Left	Right
1	62	62	137	123	16 143	15 682
2	55	65	146	124	16 681	15 075
3	74	92	148	152	14 044	13 963
4	60	61	148	131	14 951	14 389
5	56	67	125	134	15 449	16 381
6	64	74	161	119	15 144	15 550
7	50	77	124	159	13 724	15 878
8	56	52	131	133	16 795	16 203
9	55	64	115	155	16 768	16 358
10	51	70	136	120	14 043	16 026
Total	583	684	1371	1350	153 742	155 505

¹⁵ J. H. Smith, Ph.D. thesis, Cornell University, 1951 (unpublished).

¹⁶ S. D. Drell and C. L. Schwartz, Phys. Rev. **112**, 568 (1958).

¹⁷ K. W. Ford and D. L. Hill, Ann. Rev. Nuclear Sci. **5**, 25 (1955).

¹⁸ G. C. Baldwin and G. S. Klaiber, Phys. Rev. **71**, 3 (1947).

¹⁹ L. I. Schiff, Phys. Rev. **92**, 988 (1953).

TABLE II. Contributions of the uncertainties in the experimental parameters to the *fractional error* in the total number of μ^- scattering events $\Delta N/N$, and to the *absolute error* in the asymmetry ΔS .

Parameter	$\Delta N/N$ (μ^- Scat.)	$100\Delta S$ (μ^- Scat.)	$100\Delta S$ (π^- Scat.)	$100\Delta S$ (Gates)
No. 3 counter efficiency	0.15	0.10	0.10	0.10
123 coincidence efficiency	<0.02	<0.05	<0.05	<0.05
No. 4 counter efficiency	0.10	0.20	0.20	0.35
1234 coincidence efficiency	<0.01	<0.05	<0.05	<0.05
Solid angle	0.03	<0.05	<0.05	<0.05
Efficiency for decay electrons	0.02	<0.05	<0.05	
Correction for random coincidences	0.04	0.50	<0.05	<0.05
Statistical fluctuations	0.03	3.00	1.90	0.18

$N_R = 684$. A listing for each of the ten sets is given in Table I.

The only background for which the above results need to be corrected was from accidental coincidences of random counts in the No. 4 counters with the long gate ($3.00 \pm 0.10 \mu\text{sec}$) used for counting the decay electrons. This background was computed from the measured singles rates in these counters (50 ± 5)/sec, and from the duty cycle of the cyclotron. The very low value (3.0 ± 0.5) for this latter quantity was due to the use of a vibrating target in the Nevis synchrocyclotron²⁰ and resulted in the rate for accidentals of $(10 \pm 2)\%$ of the measured events.

The final results, corrected for this background, are:

$$N = 1133 \pm 60,$$

for the total number of scatterings counted;

$$S = -0.090 \pm 0.031,$$

for the left-right asymmetry.

These results can be compared with the ones obtained from the integration of the theoretical expression as discussed in Sec. IV. The yield $W = (1.1 \pm 0.1) \times 10^{-5}$ must be combined with the counted flux of $(2.0 \pm 0.3) \times 10^8$ muons and with the fraction of scatterings which yield a stopped muon count in No. 4, followed by a decay electron count. This is 0.54 ± 0.02 . The predicted results are then:

$$N = 1210 \pm 220,$$

$$S = \pm (0.081 \pm 0.001) \text{ for } \mp \mu^- \text{ helicity.}$$

In Table II we list the various contributions to the fractional error in N ; the dominant ones come from the uncertainties in detection efficiencies of the No. 3 and No. 4 counters and in the accidentals. Also listed in Table II are the various contributions to the absolute error in the asymmetry S . There, the entire error came effectively from the statistical uncertainty. This was due

to the fact that those quantities which are the same for left and right, such as No. 3 efficiency and 123 coincidence efficiency, cannot affect the asymmetry appreciably. The 1234 coincidence efficiency does not give an appreciable error because of the frequent switching of the electronic channels. The voltage setting and decay electron setting contribute only very small amounts since the No. 4 counter which is "left" for one scatterer is "right" for the next, and we have a "closed wheel" arrangement.

The significance of the agreement between the expected and the observed number of events and of the negative sign obtained for the asymmetry is discussed in Sec. VII.

VI. CHECKS

In order to check on inherent systematic asymmetries, two sets of data were used: the backward scattering of positive pions from the lead targets, and the "gate" counts produced mostly by mesonic x rays from muons which stopped in the lead.

A. π^+ Scattering

A beam of positive pions was scattered into the ten lead targets by a sheet of lead placed at the No. 2 collimator. Some of these pions could then scatter backwards and stop in the No. 4 counters. There they would decay and give a count in the delayed $3 \mu\text{sec}$ gate by the sequence $\pi^+ \rightarrow \mu^+ \rightarrow e^+$. Thus, they would simulate the true muon scattering events with the decay electron requirement, but without any left-right asymmetry. It is noted, however, that the distribution of the scattered pions is not expected to drop off as fast as the muons for the large angles in the backward scattering. Therefore, while this method is a good check insofar as asymmetries in detector efficiencies and electronic channels are concerned, it does not completely check the geometric alignment. This alignment, however, was carried out with great care using a transit and cathetometer. (Section II B.)

The left-right asymmetry obtained in this way was

$$S_{\pi^+} = +0.008 \pm 0.020,$$

where the uncertainty is essentially statistical. This is seen to be consistent with a zero systematic contribution to the measured -0.090 for the muons.

B. Gates

A further check on systematic asymmetries was available throughout the course of the experiment. This was due to the high rate of occurrence of "gate" counts: 1234 coincidences *without* the additional requirement of a delayed electron in No. 4. These counts are mainly produced by mesonic x rays which are emitted ($\approx 10^{-13}$ sec) when muons stop in the lead targets. There are also x rays from the subsequent nuclear capture of the negative muons, but this rate is negligible in the 5 nsec

²⁰ J. Rosen, Bull. Am. Phys. Soc. 6, 9 (1961).

resolving time of the $(1\bar{2}3)(4)$ coincidence. These gates are ≈ 150 times more frequent than the muon scattering events and should show a negligibly small left-right asymmetry. The value obtained was

$$S_{\text{gates}} = -0.0057 \pm 0.0039.$$

Again, this is seen to be consistent with negligible systematic contribution to the measured asymmetry.

The expected number of these gates was estimated to be $(2.5 \pm 1.0) \times 10^5$ for the total data time, in the 10 sets. The actual number measured was 3.1×10^5 .

It might be noted that in the results for gates, the uncertainties are not predominantly statistical and the systematic errors differ from those on scattering events. For gates, the No. 4 counters are required to detect electrons from x-ray conversions, and the efficiencies are more sensitive to voltages on the counters than they are for scattered muons. They differ also in that the x-ray emission is isotropic rather than peaked at smallest angles as for the muons, and therefore the counting rate is less dependent on the uncertainties in geometric alignments.

VII. DISCUSSION

As discussed in Appendix II, the negative sign for the left-right asymmetry determined by this Mott scattering experiment implies a positive helicity for the negative muon, and hence for the associated anti-neutrino, in the π^- decay. This is in agreement with $V-A$ theory and leaves unsolved the question of the identity of muon and electron neutrino. Furthermore, the experiment, in showing the agreement between the predicted and observed number of events, reinforces the conclusion that no anomaly exists in nuclear scattering,^{9,10} while in addition determines the magnitude of the asymmetry in the scattering of polarized muons to be in accord with the predicted values.

In view of the fact that the calculation for the expected yield already contains the nuclear form factor which has been measured in electron scattering experiments, we can use the present data to obtain some information on the muon charge distribution. This is done by inserting a form factor,²¹

$$f(q) = [1 + \frac{1}{6} \langle R_\mu^2 \rangle q^2]^{-1},$$

into the expression for the expected yield. An upper limit to the rms radius is obtained:

$$[\langle R_\mu^2 \rangle]^{\frac{1}{2}} < 1.9 \times 10^{-13} \text{ cm}$$

at 95% confidence level. The result is consistent with other measurements.^{9,10,22}

In principle, the data could be used to discuss the question of nuclear structure. A detailed comparison of different assumptions of nuclear shape with the experi-

ment would require more extensive calculations of the effects of variations of the parameters. A rough estimate was made by combining the calculations of reference 6 (Fermi model) with those of reference 13 which uses a uniform model.²³ The latter leads to a cross section greater by $\approx 20\%$ than the Fermi model while changing the asymmetry by less than 10%. Both possibilities fall within the uncertainties of this experiment. (The point nucleus model, however, would predict a cross section greater by a factor ≈ 20 and an asymmetry greater by a factor ≈ 4 than the measured ones.)

ACKNOWLEDGMENTS

The authors wish to express their gratitude to Professor Leon M. Lederman for his continuous guidance and encouragement; and also to thank U. Nauenberg, M. Tannenbaum, and the staff of the Nevis Cyclotron Laboratory for their assistance at various stages of the preparation of the experiment.

APPENDIX I

A beam of muons whose polarization was accurately known as a function of the kinetic energy was obtained by selecting the muons emitted near the cutoff angle in the decay in flight of pions of measured energy. The kinematics of such decays are calculated by the application of the Lorentz transformation to the Dirac-particle wave functions. It follows from this calculation that

$$\tan(\theta_s/2) = \frac{(E+m)(\gamma+1)^{\frac{1}{2}} - p(\gamma-1)^{\frac{1}{2}}}{(E+m)(\gamma+1)^{\frac{1}{2}} + p(\gamma-1)^{\frac{1}{2}}} \tan(\theta_c/2), \quad (\text{A1})$$

where, in the decay $\pi \rightarrow \mu + \nu$ of a meson moving along the z axis in the laboratory system, $\theta_c \equiv$ angle between

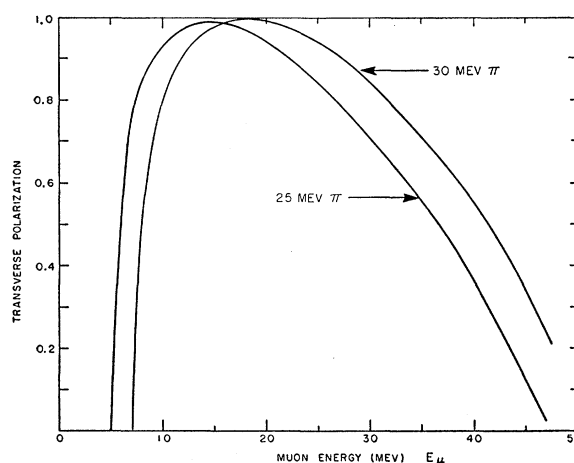


Fig. 9. Transverse polarization of muons emitted in the decay in flight of 25-Mev and 30-Mev pions, as a function of the muon energy, calculated by the application of the Lorentz transformation to the Dirac-particle wave functions (Appendix I).

²¹ S. D. Drell, Ann. Phys. (New York) 4, 75 (1958).

²² G. Charpak, F. J. M. Farley, R. L. Garwin, T. Muller, J. C. Sens, V. L. Telegdi, and A. Zichichi, Phys. Rev. Letters 6, 128 (1961).

²³ With a radius chosen such that the rms radius for the uniform distribution is the same as for the Fermi model.

the μ momentum and the z axis, measured in the rest system of the π , and $\theta_s \equiv$ angle between the μ spin direction and the z axis, measured in the laboratory system (or that angle plus 180° , depending on whether the helicity is positive or negative). E and p are the total energy and momentum of the μ in the rest system of the π . m is the mass of the μ . $\gamma = (1 - \beta^2)^{-1/2}$, where $\beta = v/c$ for the π meson, measured in the laboratory system.

The Lorentz transformation also yields, in terms of the same quantities,

$$\tan \theta_p = \frac{\sin \theta_s}{\gamma \cos \theta_s + (E/p)\beta\gamma}, \quad (\text{A2})$$

for $\theta_p \equiv$ angle between the muon momentum and the z axis, measured in the laboratory system, and

$$E_\mu = \gamma E - m + \beta \gamma p \cos \theta_s, \quad (\text{A3})$$

for $E_\mu \equiv$ kinetic energy of the muon, measured in the laboratory system.

Equations (A1), (A2), and (A3) yield a relation between E_μ and $\sin(\theta_s - \theta_p)$, which is the transverse polarization of the muons emitted in the decay in flight. This relation is shown plotted in Fig. 9 for two values of the kinetic energy of the π mesons at decay.

APPENDIX II

Although it is necessary to consider the phase shift calculation^{6,13} to relate the asymmetry in Mott scattering of a transversely polarized charged particle to its spin direction, the following simple model gives the correct sign relationship:

Consider a negative muon and a nucleus passing each other in the two cases shown in Fig. 10. The spin is shown "up" in both cases (positive helicity) and thus the magnetic moment is "down" for these negative charges, corresponding to clockwise currents viewed from above. In (a) the muon is passing to the right of the nucleus, in (b) to the left. The situation is clearly

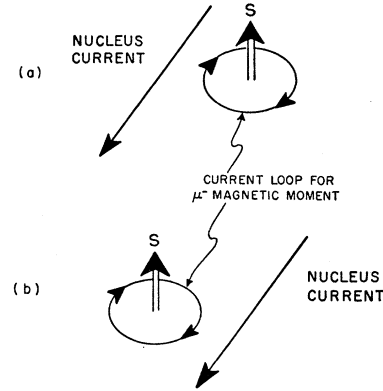


FIG. 10. Scattering of a muon by a nucleus, represented by the equivalent picture of a muon at rest and a positive nucleus current in the direction opposite to original muon momentum. Both cases are shown with spin "up" (positive helicity for transversely polarized muon) and with the current loops corresponding to the μ^- magnetic moment. In (a) the muon is passing to the right of the nucleus, and hence experiences a net force to the right for the repulsion of antiparallel currents. In (b) the muon is passing to the left, and experiences a force to the right for parallel currents. Thus, in both cases there is an enhancement to the right for positive helicity.

analogous to the muon at rest—a clockwise current—and the positively charged nucleus moving in the direction opposite to the original direction of the muon. Then (a) is seen to correspond to two antiparallel currents, or a repulsion of the muon toward the right; and (b) shows two parallel currents, an attraction of the muon toward the right. It follows that an enhancement to the right is expected for positive-helicity negatively charged particles, or negative asymmetry

$$S = (\text{Left} - \text{Right}) / (\text{Left} + \text{Right}).$$

It is noted that these directions are unambiguously defined in the usual orthogonal coordinate system of Sec. I as the x axis for "left," where the spin is along y (for positive helicity) and the incoming muon momentum is along z .